Journal of Materials Chemistry B

Selective Fluorescence Detection of Proteins Using Molecularly Imprinted Hydrogels with Aggregation-Induced Emission

Journal:	*Journal of Materials Chemistry B*
Manuscript ID	TB-ART-01-2025-000170.R1
Article Type:	Paper
Date Submitted by the Author:	11-Apr-2025
Complete List of Authors:	Kubo, Takuya; Kyoto Prefectural University, ; Kyoto University, Kako, Kankichi; Kyoto University, Kanao, Eisuke; Kyoto University, Graduate School of Pharmaceutical Sciences; National Institute of Biomedical Innovation Health and Nutrition, Ishihama, Yasushi; Kyoto University Konishi-Yamada, Sayaka; Kyoto Prefectural University

ARTICLE

Selective Fluorescence Detection of Proteins Using Molecularly Imprinted Hydrogels with Aggregation-Induced Emission

Received 00th January 20xx,
Accepted 00th January 20xx

DOI: 10.1039/x0xx00000x

Kankichi Kako,[a] Eisuke Kanao,[b,c] Yasushi Ishihama,[b] Sayaka K-Yamada,[d] Takuya Kubo*[,a,d]

Molecular imprinting is known as a method for synthesizing materials that selectively adsorb specific molecules. The polymers obtained by this method are inexpensive, highly chemically stable, and easy to prepare, but there is a problem that definite and easy detection for the adsorption of target molecules is difficult. We aimed selective fluorescence detection of proteins by introducing fluorescent molecules into a molecularly imprinted hydrogel (MIH). For fluorescence detection, we used aggregation-induced emission (AIE), which has been attracting attention in recent years. Molecules exhibiting AIE have the characteristic that their fluorescence intensity increases due to factors such as aggregation of molecules or chemical interaction with target molecules. New AIE monomer was synthesized, and its characteristics were evaluated. The MIHs were prepared with an AIE monomer, functional monomers, poly(ethylene glycol) diacrylate as a crosslinker, and lysozyme as a target protein. The MIH showed selective adsorption for lysozyme and a specific increase in fluorescent intensity. Even in a protein mixture sample, we achieved optical detection for lysozyme.

1. Introduction

Protein analysis plays a critical role in a wide range of fields from medical diagnosis to environmental investigation; especially, enzyme-linked immunosorbent assay (ELISA) is a commonly applied diagnostic test using antibody-antigen reaction. ELISA offers high specificity and sensitivity,[1-7] while the assay procedure is time-consuming and it is comparatively expensive. In this study, we aim to develop a detection method selectively absorbing proteins and making fluorescence increase, trying to solve problems above by employing molecularly imprinting technology due to its simple procedure. Furthermore, application of aggregation-induced emission (AIE)[8-12] may not only enable more accurate detection but also contribute to development of wide variety of usages as an innovative fluorescent detection method. Molecularly imprinted hydrogel (MIH) is a macromolecular material selectively adsorbing target molecules.[13-20] MIH is prepared as following procedures: a hydrogel is fabricated by incorporating target molecules as templates, and after washing to remove the template molecule, molecular recognition site is formed. It holds specific properties as duplicating the key hole of molecular shape for a template molecule by three dimensionally arranging functional monomers in precise. MIH is applied to a wide variety of fields, not only analytical chemistry but also drug delivery and medical diagnosis, since it is easily fabricated at low cost and chemically stable. As hydrogels have flexible structures, they have been commonly used for analysis of biomacromolecules such as protein having complex structures. Especially, in our previous studies, MIH with a poly(ethylene glycol) (PEG)-based cross-linker has been examined because of its property suppressing non-specific adsorption of a target protein.[21-26] However, there is a drawback in MIH that visible detection of absorption of a target molecule is hardly achieved.

To solve the problem, we attempted to introduce fluorescent molecules, showing AIE to MIH for the specific interaction with the target protein (Figure 1). The fluorescent molecules showing AIE emit in the aggregate state, preventing concentration quenching. Because of this advantage, they have drawn attention lately as the molecules solving the drawbacks of general fluorescent molecules. The typical examples of the molecules showing AIE are tetraphenylethylene and trans-phenylstilbene. These molecules consume excitation energy because of intramolecular free rotation of aromatic rings in the spread state. On the contrary, in the aggregate state, excitation energy is emitted as intramolecular free rotation is suppressed by stacked aromatic rings.[27-30] Aside from this aspect, when the fluorescent molecules interact with the target molecules such as proteins, fluoresce intensity increases, which process is not related with aggregation of the fluorescent molecules, but some articles reported this phenomenon as AIE broadly speaking.[31, 32]

In this study, firstly, we synthesize a fluorescent monomer (Figure 2), which shows AIE, for introducing MIH. The monomer involving anionic functional groups was prepared under the assumption that AIE emerges interacting with amino-acid residues of the target template molecule. We supposed that the fluoresce intensity increases when the target protein adsorbs to MIH by introducing the fluorescent monomer to MIH.

[a] *Graduate School of Engineering, Kyoto University, Katsura, Nishikyo-ku, Kyoto 615-8510, Japan*
[b] *Graduate School of Pharmaceutical Sciences, Kyoto University, Sakyo-ku, Kyoto 606-8501, Japan*
[c] *National Institutes of Biomedical Innovation, Health and Nutrition, Ibaraki, Osaka 567-0085, Japan*
[d] *Graduate School of Life and Environmental Science, Kyoto Prefectural University, 1-5 Shimogamo Hangi-cho, Sakyo-ku, Kyoto 606-8522, Japan*
† Footnotes relating to the title and/or authors should appear here.
Electronic Supplementary Information (ESI) available: [details of any supplementary information available should be included here]. See DOI: 10.1039/x0xx00000x

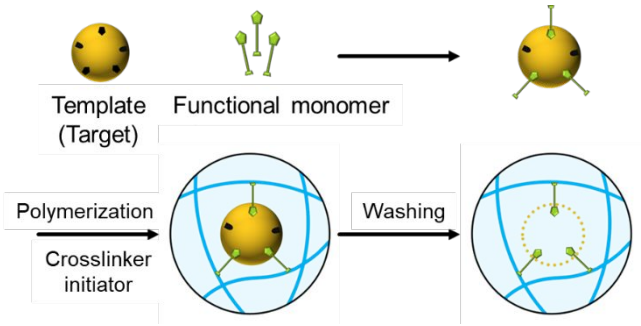

Figure 1. Concept of a molecularly imprinted hydrogel for the fluorescence detection.

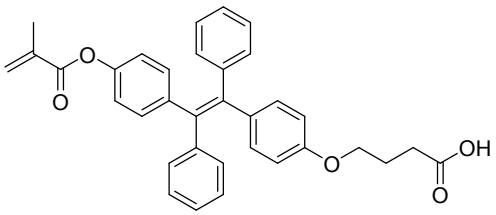

Figure 2. Structure of the fluorescent monomer.

2. Materials and method

2.1 Synthesis of fluorescent monomers showing AIE

As shown in Scheme 1, 4,4'-(1,2-Diphenylethene-1,2-diyl) diphenol (cis- and trans- mixture) (DPEDDP) 160 mg, NEt_3 120 µL, and CH_2Cl_2 12 m L were added in a 100 mL eggplant flask, and 28 µL of methacryloyl chloride was dripped being shaken in an ice bath. Then it was shaken for 5 h at room temperature, diluted with saturated NaCl aqueous solution of 50 mL, extracted with CH_2CI_2. Dehydration with magnesium sulfate (anhydrous) was conducted, followed by evaporation. Then a yellow solid was precipitated. The yellow solid of 65 mg, 4-dimethylaminopyridine of 0.35 mg, NEt3 of 31.9 µL, and CH_2Cl_2 of 12 mL were added in a 100 mL eggplant flask, and succinic anhydride of 20 mg was added being shaken. The mixture solution was reacted for 12 h at room temperature. After that, the solution was diluted with saturated NaCl aqueous solution of 50 mL, extracted with $CHCl_3$. After dehydration with magnesium sulfate (anhydrous) and evaporation were conducted, the yellow solid was precipitated. In each reaction, progression of reaction was examined by thin layer chromatography (TLC), and then purification was conducted using silica gel chromatography. Finally, the fluorescent monomer of 92 mg was obtained (recovery rate 40.3 %).

2.2 Evaluation of effects for fluorescent intensity at the various ratios of organic solvents and different concentrations of proteins

The solution of the AIE monomer of 100 µM was prepared at the ratio of organic solvents 10-60 % using dimethyl sulfoxide (DMSO) or acetonitrile as an organic solvent with water. Fluorescent spectra of the solution were then measured using the plate reader.

Highly hydrophobic protein BSA and basic protein lysozyme, which easily interact with the carboxyl groups of the AIE monomer, were utilized as target proteins. The fluorescent spectra were measured when the protein was added in the solution dissolved the AIE monomer of 100 µM. We also evaluated effects at different concentrations of the proteins in a hydrogel. Hydrogels were prepared with lysozyme, the AIE monomer, 14G', NIPAAm, MAA, and APS at 0-80 µM, 100 µM, 30 mM, 1200 mM, 35 mM, and 0.1w/v% (vs. crosslinkers), respectively. Then TEMED was added to be 0.1 vol% (vs. solution), and the solution was moved to a 1 mL syringe tube for polymerization. After 24h, the hydrogel was removed from the syringe tube, cut by 2 mm in thickness. The gel tips were placed on a well plate, and the fluorescence intensity was measured by the plate reader (excitation: 320 nm, fluorescence: 480 nm).

2.3 Evaluation of adsorption specificity of a MIH and a NIH containing NIPAAm

The hydrogel containing NIPAAm was fabricated, and the fluorescence intensity when proteins adsorb to the NIH was evaluated. We expected that the hydrogels are reversibly swelled and shrunk by interaction of NIPAAm. The NIH was prepared with the AIE monomer, 14G', NIPAAm, MAA, and APS at 100 µM, 30 mM, 1200 mM, 35 mM, and 0.1w/v% (vs. 14G' + NIPAAm), respectively. Then TEMED was added to be 0.1v/v% (vs. solution), and the solution was moved to a 1 mL syringe tube for polymerization. After 24h, the hydrogel was removed from the syringe tube, sliced by 2 mm in thickness. The sliced gel tips were washed with 1 M NaCl aq., replaced with 1 mM tris-HCl buffer. After they were immersed in 0-200 µM lysozyme aq., the adsorption amount and the fluorescence intensity were measured. In addition, MIH was fabricated by adding lysozyme to the same solution as the NIH to be 0.8 mM. After the MIH was washed under the same condition with NIH, immersed in 50 mM NaCl + 1 mM tris-HCl aq. Adsorption specificity was evaluated through the protein adsorption.

2.4 Evaluation of the MIH after optimizing the composition

To improve adsorption specificity, optimization of the composition was implemented. Lastly, the MIH was prepared with lysozyme, the AIE monomer, 14G', NIPAAm, AMPS, SS, and AIZP at 0.38 mM, 100 µM, 42.7 mM, 292 mM, 5.7 mM, 1.13 mM, 0.5w/w% (vs. 14G' + NIPAAm), respectively. The solution was moved to a 3 mL pyrex tube and irradiated UV at 365 nm for 4 h to be polymerized. Then the prepared hydrogel was cut by 2mm in thickness, washed with 1 M NaCl aq., and

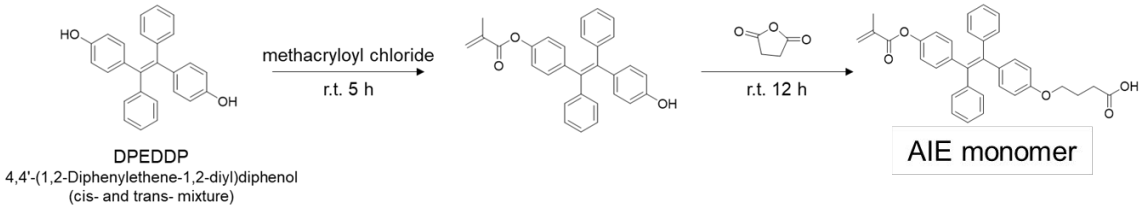

DPEDDP
4,4'-(1,2-Diphenylethene-1,2-diyl)diphenol
(cis- and trans- mixture)

Scheme 1. Synthesis of fluorescence monomers.

immersed in 50 mM NaCl + 1 mM tris-HCl aq. Then the gel tips were immersed in 0-30 μM lysozyme, an adsorption amount and the fluorescence intensity were measured. Additionally, an adsorption experiment using BSA, cytochrome c, trypsin was also conducted.

2.5 Evaluation of the MIH washed using basic solvents

The MIH was prepared with lysozyme, the AIE monomer, 14G', AMPS, SS, AIZP at 0.38 mM, 100 μM, 85.3 mM, 5.7 mM, 1.13 mM, 0.5w/w% (vs. 14G'), respectively. The solution was moved to a 3 mL pyrex tube, irradiated with UV light for 4 h for polymerization. Then the hydrogel was sliced by 2 mm in thickness, washed with 1 M NaCl aq. and 0.1% triethylamine aq., replaced with 50 mM NaCl + 1 mM tris-HCl aq. Lastly, the adsorption amount and the fluorescence intensity were measured after immersing the MIH and the NIH in 0-40 μM lysozyme. At the same time, the adsorption experiment was implemented using BSA, cytochrome c, and trypsin.

3. Results and discussion

3.1 Synthesis of the AIE monomer

A Figure S1 (a) shows the obtained result of a start compound and products after reaction at the first step by TLC. In addition to monosubstituted products, disubstituted products were observed. Figure S1 (b) shows the obtained result of monosubstituted products and products after reaction at the second step by TCL. Production of fluorescent monomers was observed.

Furthermore, the 1H-NMR spectrum shown in Figure S2 indicates purification of the objective. According to the NMR analysis, we successfully synthesized a fluorescent monomer, tetraphenylethylene derivative, from DPEDDP.

3.2 Fluorescent characteristics for the synthesized AIE monomer

Figure 3 shows the fluorescent spectra evaluating effects at various ratios of the organic solvents in the solution dissolved a fluorescent monomer of 100 μM. In both cases of DMSO and acetonitrile, the fluorescence intensity increased as the ratio of organic solvents decreased. This can be explained that when the ratio of organic solvents decreased, AIE was emerged by aggregation of the fluorescent monomers caused by hydrophobic interaction. Besides, the fluorescent monomers may tend to aggregate more in DMSO than in acetonitrile.

Figure 4 shows the fluorescent spectra evaluating effects at different concentrations of the proteins in the solution dissolved a fluorescent monomer of 100 μM. When BSA was added, the fluorescence intensity increased in accordance with an increase in the concentration of BSA. On the contrary, when lysozyme was added, the fluorescence intensity did not increase. According to these results, AIE can be emerged by hydrophobic interaction between BSA and the fluorescent monomers in the solution, but AIE may not emerge due to electrostatic interaction with lysozyme.

Figure S3 shows fluorescence intensity of the hydrogels using the AIE monomer with different concentrations of the proteins. Unlike in the solution, the fluorescence intensity increased in accordance with an increase in the concentration of lysozyme in the hydrogel. This is because the fluorescent monomers do not freely move as crosslinked in the hydrogel so that intermolecular rotation may be easily hampered even during electrostatic interaction with the proteins. This phenomenon suggests possibility of fluorescence detection using MIH introduced the fluorescent monomers. These suggest that the synthesized fluorescent monomer shows features of AIE. Taken together, the fluorescence intensity can increase by adsorbing proteins to MIH introduced the fluorescent monomers.

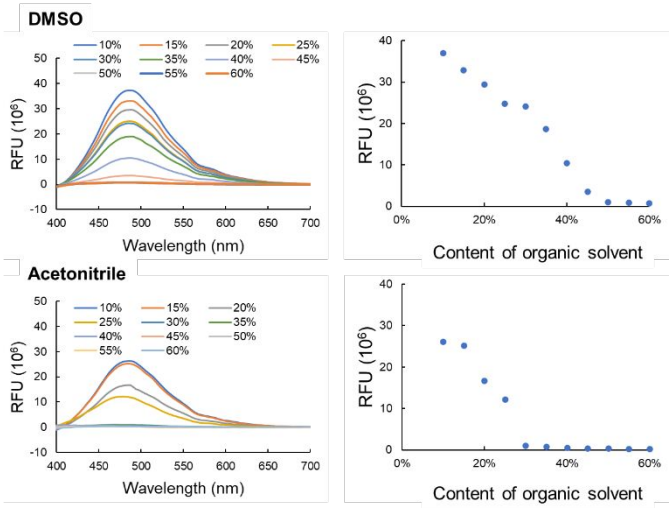

Figure 3. Evaluation of the fluorescent intensity of the synthesized AIE monomer at various ratios of the organic solvents, top, DMSO; bottom, acetonitrile.

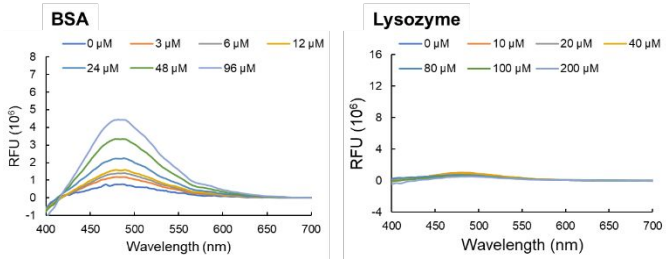

Figure 4. Evaluation of the fluorescent intensity of the synthesized AIE monomer at different concentrations of the proteins, left, BSA; right, lysozyme.

3.3 Evaluation of fluorescence MIH introduced NIPAAm

Herein change in the fluorescence intensity on protein re-adsorption to the hydrogels that were washed to remove proteins was evaluated. We consider a condition where the fluorescence intensity increases by adsorbing proteins to the prepared hydrogels. For enhancing AIE phenomenon, NIPAAm was applied to MIHs. Normally, polymers including NIPAAm show a thermo-responsive characteristic, showing hydrophobicity over lower critical solution temperature. Similarly, we expected the dehydrate polymers including NIPAAm show hydrophobicity, causing aggregation by hydrophobic interaction.[33] Considering this feature, in our case, the MIHs may hydrophobically

shrink with the fluorescent monomer when a target protein adsorbs, leading to effective fluorescent detection.

Figure 5 shows the result of the lysozyme adsorption experiment using the NIH. In accordance with lysozyme adsorbing to the NIH, the hydrogel shrunk, and the fluorescence intensity increased. This result suggested that lysozyme adsorbing to the hydrogel led dehydration, resulting in aggregation caused by hydrophobic interaction with NIPAAm and emergence of AIE. Furthermore, Figure S4 shows the result of the amount of lysozyme adsorption to both the MIH and the NIH. NaCl was added to the adsorption solution to inhibit non-specific adsorption, but adsorption specificity was not observed. This may be because the excessive amount of NIPAAm increased non-specific adsorption, and the template molecule, lysozyme, was not completely washed with this composition. In fact, 60% of lysozyme remained in the MIH without being removed by washing (Figure S4-b).

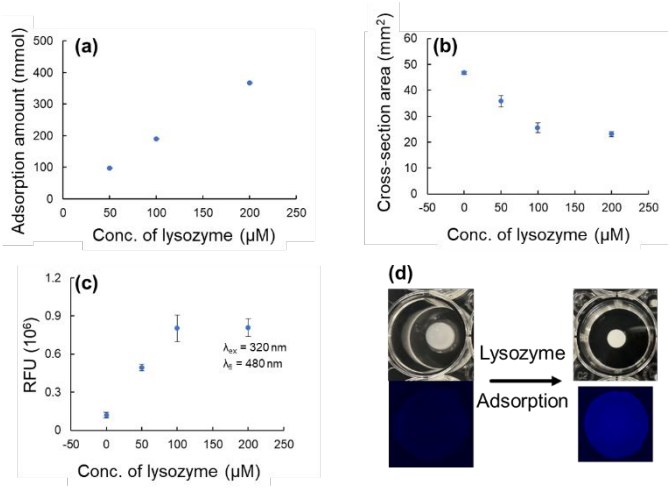

Figure 5. (a) Amount of lysozyme adsorption to the NIH, (b) cross-sectional area, (c) integrated fluorescence intensity of cross-section, (d) fluorescent microscope images of before adsorption and after adsorption. (*n*=3)

3.4 Evaluation of the MIH after optimizing the composition

As shown in Figure 6, the removed lysozyme by washing was significantly improved in the MIH that the composition was optimized as experimental, 2.4. Furthermore, the adsorption selectivity of MIH toward lysozyme was more than twice as high as that of NIH. It can be caused by the following factors: (1) the less amount of NIPAAm decreased non-specific adsorption, (2) density of the cross-linked network of polymer structures decreased as initiator was optimized. At the same time, the degree of an increase in the fluorescence intensity of the MIH was not as high as previous one, while the fluorescence intensity of NIH did not change. Furthermore, both the MIH and the NIH shrunk in line with adsorption. According to these results, the MIH showed the selective adsorption of a target protein, lysozyme, and its fluorescent detection, although it was difficult to be visually detected.

Figure S5 shows the result of an adsorption experiment using various proteins. Higher adsorption amount and imprinting factor toward lysozyme was observed. Regarding the fluorescence intensity of cytochrome c, as the wavelength of fluorescence was like absorption wavelength of cytochrome c, data was not accurately obtained. Among other proteins, the fluorescence intensity clearly increased when the MIH adsorbed lysozyme. According to these results, we successfully prepared the MIH showing selective adsorption and fluorescent detection toward the target protein. Adsorption specificity to the adsorption amount and fluorescence intensity and selectivity to various proteins were observed by optimizing the composition. However, there was a challenge that fluorescence intensity was too small to be visually detected.

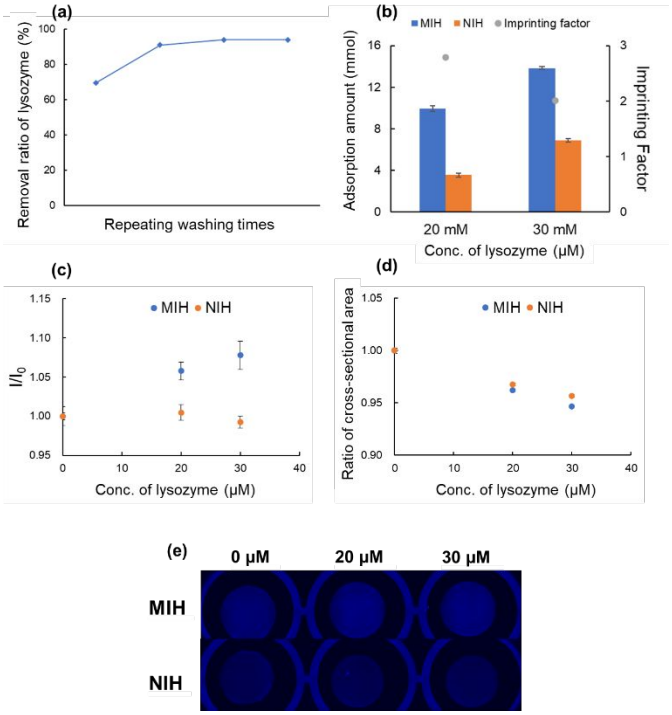

Figure 6. Evaluation of MIH after optimizing the composition, (a) template removal ratio, (b) adsorption amount, (c) fluorescence intensity, (d) ratio of cross-section area, (e) fluorescence microscope image. (*n*=3)

3.5 Evaluation of fluorescent MIH washed with basic solutions

While adsorption specificity on the MIH containing the fluorescent monomer and NIPAAm was observed as the fluorescent intensity increased, the absolute fluorescence intensity was too weak to be visually detected. Figure S6 shows the fluorescence intensity of the MIHs and NIHs before and after washing. Here, the images of each hydrogel were loaded by a fluorescence microscope, then the images were processed by ImageJ and the brightness of only blue was estimated throughout the cross-section as an average value (B Value, n = 4). The intensity on the NIH was almost same whether the NIHs were washed or not. In contrast, the fluorescence intensity of the MIH was high even before and after washing, regardless of whether NIPAAm existed or not. Ideally, the fluorescence intensity of the MIH should be equivalent to that of the NIH after washing. This may be because unwashed lysozyme interacted with the fluorescent monomer or even though all lysozymes had been

washed, fluorescent monomers at around a molecular recognition site interacted each other. Thus, we attempted to further wash with triethylamine for possibly leading to substitution of triethylamine with remained lysozyme. As well as triethylamine may ionize carboxyl groups of the fluorescent monomer, which causes electrostatic repulsion among the fluorescent monomers. In addition, we envisaged that interaction between the hydrophobic part of NIPAAm and lysozyme may be the obstruction for washing lysozyme so that evaluation of the MIH was conducted without using NIPAAm.

Figures 7(a,b) show the ratio of cross-section area of the MIH compared to before washing and the fluorescence intensity when washing with the basic solvent. The MIH swelled by washing with the basic solvent, which decreased the fluorescence intensity. This can be explained that further washing with triethylamine led to substitution of triethylamine with remained lysozyme and ionization of carboxyl groups of the fluorescent monomer, which caused electrostatic repulsion among the fluorescent monomers.

Figures 7(c, d) show the result of the adsorption experiment using the MIH and the NIH toward lysozyme. Adsorption specificity of lysozyme on the MIH decreased when washing with the basic solvent compared with when not washing. It can be explained that washing with the basic solvent ionized acidic functional groups of the functional monomer, which augmented non-specific adsorption on the NIH. At the same time, as the adsorption amount of both the MIH and the NIH increased, the fluorescence intensity also remarkably increased. Especially, the fluorescence intensity of the MIH increased by over 15% and it was visually detected, while the increase in fluorescence intensity became moderate at over concentration of lysozyme, 20 µM. This may be because this concentration of lysozyme is equivalent to the number of the specific recognition sites in the MIH, and non-specific adsorption relatively became large at over 20 µM; therefore, adsorption selectivity became diminished.

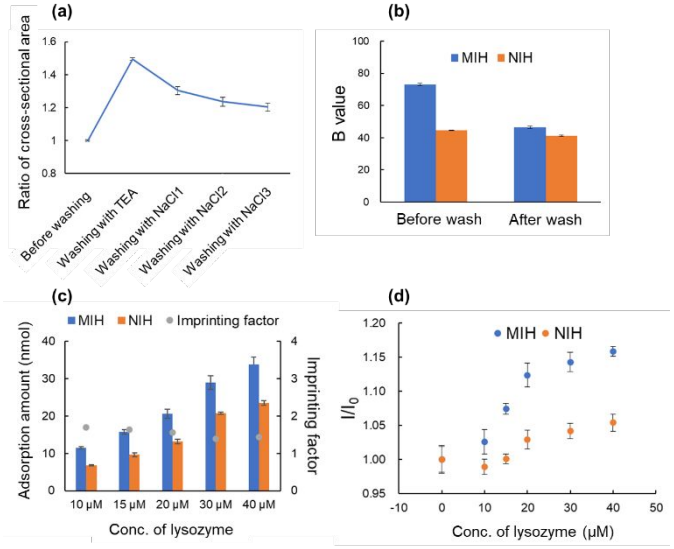

Figure 7. (a) Ratio of cross-section area of the MIH while washing, (b) fluorescence intensity before and after washing with triethylamine aq. and results of the adsorption experiment using the MIH and the NIH toward lysozyme, (a) adsorption amount of lysozyme, (b) fluorescence intensity. (*n*=3)

Figure 8(a, b) shows the result of the adsorption experiment using various proteins. Adsorption specificity on the MIH toward lysozyme was observed but no other proteins, and the fluorescence intensity obviously increased with only the MIH adsorbing lysozyme. This result also suggests that the fluorescence intensity effectively increased when the template protein was adsorbed to the specific recognition sites in the MIH. As described above, the decrease in the fluorescence intensity with the gels adsorbing cytochrome c can be explained that the wavelength of fluorescence was like absorption wavelength of cytochrome c. Furthermore, Figure 8 (c, d) shows the result of the adsorption experiment using a mixed analyte. Even with contaminant proteins, high selectivity was observed without damaging specific adsorption toward lysozyme.

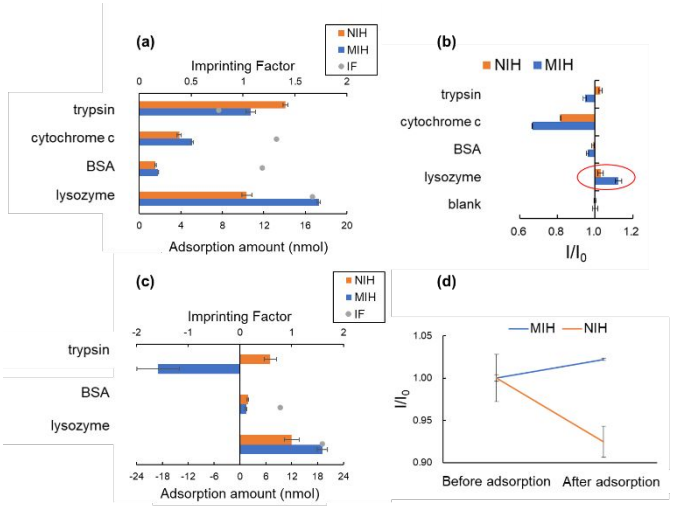

Figure 8. Evaluation of adsorption selectivity using proteins, (a) adsorption amount, (b) fluorescence intensity, (b) fluorescent intensity (with single analyte), and evaluation of selectivity using a mixed analyte, (c) adsorption amount, (d) fluorescence intensity. (*n*=3)

Conclusions

In this study, we aimed selective fluorescence detection of target proteins by applying AIE to MIHs. We synthesized a fluorescent monomer that shows AIE and it increased in line with a decrease in the organic solvent ratio and an increase in the protein concentration, suggesting that the monomer has an AIE function. We fabricated and evaluated the AIE-introduced MIH containing NIPAAm. Addition of NIPAAm resulted in shrinkage and an increase in fluorescence when proteins were adsorbed, suggesting the possibility of fluorescence detection. However, problems arose due to the addition of NIPAAm, such as an increase in nonspecific adsorption and a decrease in specificity, and a small increase in fluorescence, making it difficult to detect visually. The purpose of washing with basic solutions is to wash away the template protein slightly remained and eliminate the aggregated fluorescent monomers near the imprinted space, and during the washing process, the fluorescence intensity of MIH reached as same level as that of NIH. The MIH showed a remarkable increase in fluorescence upon adsorption of the target protein, demonstrating high selectivity compared to other proteins. We believe that our

method enables to clearly visualize target protein adsorption, which is difficult with conventional molecular imprinting methods.

Author Contributions

All authors contributed to and have given approval for the final version of the manuscript. T. Kubo supervision, project administration, funding acquisition, conceptualization, methodology, writing-original draft, writing-review & editing; K. Kako, E. Kanao, Y. Ishihama conceptualization, data curation, formal analysis, S. K-Yamada writing-original draft, writing-review & editing.

Conflicts of interest

There are no conflicts to declare.

Acknowledgements

This work was partly supported by JST, CREST Grant Number JPMJCR2332, JST A-STEP Grant Number JPMJTR214C, and the Environment Research and Technology Development Fund (JPMEERF20235003) of the Environmental Restoration and Conservation Agency of Japan.

References

1. S. Balayan, N. Chauhan, W. Rosario and U. Jain, *Appl. Surf. Sci. Adv.*, 2022, **12**, 100343.
2. A. K. Barik, C. Mathew, P. M. Sanoop, R. V. John, S. S. Adigal, S. Bhat, K. M. Pai, S. V. Bhandary, T. Devasia, R. Upadhya, et al., *J. Chromatogr. B. Biomed. Appl.*, 2024, **1232**, 123944.
3. H. Liu, J. J. Song, Z. Y. Zhao, S. Q. Zhao, Z. Y. Tian and F. Yan, *Adv. Sci.*, 2024, **11**, 2305347.
4. H. Noji, Y. Minagawa and H. Ueno, *Lab Chip*, 2022, **22**, 3092-3109.
5. P. Peng, C. Liu, Z. D. Li, Z. R. Xue, P. Mao, J. Hu, F. Xu, C. Y. Yao and M. L. You, *Trac-Trend. Anal. Chem.*, 2022, **152**, 116605.
6. A. Varesi, A. Carrara, V. G. Pires, V. Floris, E. Pierella, G. Savioli, S. Prasad, C. Esposito, G. Ricevuti, S. Chirumbolo, et al., *Cells*, 2022, **11**, 1367.
7. Y. Zhang, Q. Li and B. Zhang, *Crit. Rev. Anal. Chem.*, 2024, DOI: 10.1080/10408347.2024.2379853, 1-11.
8. M. Bayat, H. Mardani, H. Roghani-Mamaqani and R. Hoogenboom, *Chem. Soc. Rev.*, 2024, **53**, 4045-4085.
9. M. H. Chua, K. L. Chin, X. J. Loh, Q. Zhu and J. W. Xu, *ACS Nano*, 2023, **17**, 1845–1878.
10. Y. H. Liu, X. Q. Chen, X. T. Liu, W. J. Guan and C. Lu, *Chem. Soc. Rev.*, 2023, **52**, 1456-1490.
11. H. R. Wang, Q. Y. Li, P. Alam, H. T. Bai, V. Bhalla, M. R. Bryce, M. Y. Cao, C. Chen, S. J. Chen, X. R. Chen, et al., *ACS Nano*, 2023, **17**, 14347-14405.
12. F. Y. Zhu, L. J. Mei, R. Tian, C. Li, Y. L. Wang, S. L. Xiang, M. Q. Zhu and B. Z. Tang, *Chem. Soc. Rev.*, 2024, **53**, 3350-3383.
13. A. Balakrishnan, S. Appunni, M. Chinthala, M. M. Jacob, D. V. N. Vo, S. S. Reddy and E. S. Kunnel, *Environ. Chem. Lett.*, 2023, **21**, 1881-1905.
14. H. R. Culver, J. R. Clegg and N. A. Peppas, *Acc. Chem. Res.*, 2017, **50**, 170-178.
15. M. C. Koetting, J. T. Peters, S. D. Steichen and N. A. Peppas, *Mater. Sci. Eng. R Rep.*, 2015, **93**, 1-49.
16. S. Ramanavicius, A. Jagminas and A. Ramanavicius, *Polymers*, 2021, **13**, 974.
17. S. Ramanavicius and A. Ramanavicius, *Polymers*, 2021, **13**, 49.
18. J. Sarvutiene, U. Prentice, S. Ramanavicius and A. Ramanavicius, *Biotechnol. Adv.*, 2024, **71**, 108318.
19. W. X. Tang, L. Yin, J. R. Sempionatto, J. M. Moon, H. Teymourian and J. Wang, *Adv. Mater.*, 2021, **33**, 2008465.
20. C. C. Villa, L. T. Sánchez, G. A. Valencia, S. Ahmed and T. J. Gutiérrez, *Trends Food Sci. Technol.*, 2021, **111**, 642-669.
21. E. Kanao, Y. Tsuchiya, K. Tanaka, Y. Masuda, T. Tanigawa, T. Naito, T. Sano, T. Kubo and K. Otsuka, *ACS Appl. Polym. Mater.*, 2021, **3**, 226-232.
22. T. Kubo, S. Arimura, Y. Tominaga, T. Naito, K. Hosoya and K. Otsuka, *Macromolecules*, 2015, **48**, 4081-4087.
23. T. Kubo, H. Furuta, T. Naito, T. Sano and K. Otsuka, *Chem. Commun.*, 2017, **53**, 7290-7293.
24. T. Kubo, N. Watanabe, S. Ikari, C. C. Liu, E. Kanao, T. Naito, T. Sano and K. Otsuka, *Anal. Methods*, 2021, **13**, 3086-3091.
25. C. C. Liu, T. Kubo and K. Otsuka, *J. Mater. Chem. B*, 2022, **10**, 6800-6807.
26. Y. Manmana, N. Hiraoka, T. Naito, T. Kubo and K. Otsuka, *J. Mater. Chem. B*, 2022, **10**, 6664-6672.
27. J. K. Liu, H. K. Zhang, L. R. Hu, J. Wang, J. W. Y. Lam, L. Blancafort and B. Z. Tang, *J. Am. Chem. Soc.*, 2022, **144**, 7901-7910.
28. S. J. Liu, Y. Y. Li, R. T. K. Kwok, J. W. Y. Lam and B. Z. Tang, *Chem. Sci.*, 2021, **12**, 3427-3436.
29. Y. Z. Shi, H. Wu, K. Wang, J. Yu, X. M. Ou and X. H. Zhang, *Chem. Sci.*, 2022, **13**, 3625-3651.
30. C. Wang, W. J. Chi, Q. L. Qiao, D. V. Tan, Z. C. Xu and X. G. Liu, *Chem. Soc. Rev.*, 2021, **50**, 12656-12678.
31. S. Zang, S. Wu, L. Xiao, X. Deng and Y. Zhao, *Anal. Chem.*, 2022, **94**, 8365-8372.
32. K. Krishnaveni, S. Gurusamy, V. Sathish, P. Thanasekaran and A. Mathavan, *Spectrochimica Acta Part A: Molecular and Biomolecular Spectroscopy*, 2021, **252**, 119537.
33. N. Adrus and M. Ulbricht, *Polymer*, 2012, **53**, 4359-4366.

Data are available upon request from the authors.